SAE INTERNATIONAL

# Distribution of Cooling Structures in Water Cooled Electrical Machines using Localized Loss Profiles

2023-24-0126

Published: August 28, 2023

**Christoph Ellenrieder[1], Benedikt Reick[1], and Marcus Geimer[2]**
[1]Ravensburg-Weingarten University
[2]Karlsruhe Institute of Technology

**Citation:** Ellenrieder, C., Reick, B., Kaufmann, A., and Geimer, M., "Distribution of Cooling Structures in Water Cooled Electrical Machines Using Localized Loss Profiles," SAE Technical Paper 2023-24-0126, 2023

DOI: https://doi.org/10.4271/2023-24-0126

Received: 31 Jul 2023 Revised: 31 Jul 2023 Accepted: 07 Jul 2023

## Abstract

Cooling is a critical factor for improving power density in electrical appliances, especially in integrated drives for mobile applications. However, the issue of distributed losses in electric machines can lead to hotspots and temperature gradients within the electric drive. Traditional cooling jackets use unidirectional flow without or with evenly distributed cooling structures. This often aggravates the issue of hotspots, resulting in thermal derating and thus limiting the operation range. As well, a non-demand oriented distribution of cooling structures leads to unnecessary pressure losses.

This problem is addressed with a newly elaborated method for distributing cooling elements, i.e., pin fins with varying density distribution inside the cooling channel. Results from previous work, numerical simulations, and measurement data from a planar test bench are used. The approach segments the cooling channel by using a loss profile. This profile and analytic heat transfer calculations are used to determine the required density of cooling elements for dissipating the locally induced losses. For a linear channel with uniformly distributed losses, this results in an increasing number of cooling elements within the channel in fluid flow direction. With localized losses, this will result in an increased density distribution in the respective areas. The method is evaluated by applying it to a planar test channel and investigating the temperature distribution on a test bench. First results indicate that the newly developed cooling element distribution provides an advantageous temperature distribution. The temperature gradient along the cooling channel shows a reduction from 23 K to 9 K with the distributed cooling elements.

The method, previously tested in the linear planar channel, then is applied to the construction of a cooling jacket with a specifically designed two-layer cooling channel. This design is analyzed using CFD, a prototype is currently under production. Tests on the prototype will follow in further investigations.

## Introduction

The design and operation of electrical machines are increasingly important for a sustainable and energy-efficient future. The percentage of registered passenger battery electric vehicles (BEVs) in the EU increased from 0.25 % in 2019 to 1.19 % in 2022, and for light commercial BEVs from 0.34 % to 0.75 %. This trend is following exponential growth [1] and is driven by regulations and subsidies related to the ecological impact. To further increase the adoption of BEVs, electric drives must become cheaper and more compact. The efficient conversion of electrical energy into mechanical energy is critical for applications such as electric vehicles, industrial machinery, and mobile working machinery [2]. However, electrical machines generate heat during operation, which can negatively impact performance, reliability, and service life. Therefore, thermal management of electrical machines is an important consideration for their design and operation. Integrated drives, where power electronics and electric motors are spatially integrated, have been recognized as an effective approach for addressing the increasing demand for more compact and efficient electric drives. In addition, as electric machines are becoming more powerful and compact, the issue of thermal management becomes increasingly significant [3]. One of the key challenges is to manage the thermal effects of distributed losses in the machine, which can lead to temperature gradients along the cooling channels and affect the overall performance and reliability of the system [4–7]. These challenges are addressed by various works summarized in [3], various cooling techniques have been proposed, including liquid cooling, air cooling, and hybrid cooling. Liquid cooling, in particular, has gained significant attention due to its high cooling efficiency and ability to remove heat from high-power density applications. In liquid cooling, a cooling fluid, such as water or oil, is circulated through a cooling channel that is integrated into the housing, and absorbs the heat generated by the machine.

With those increasing requirements, different domains have to be considered in the design of an electric drive, and in particular, the electric motor:

- Mechanical transmission of forces
- Electromagnetic generation of forces
- Thermal stability of materials

To ensure the fulfillment of these requirements, Finite Element Method (FEM) tools are used. However, FEM simulations are time-consuming and can result in slow iterations, leading to delays in the design process. Additionally, there is currently no method for cooling jackets to address the problem of distributed losses, which can significantly impact the performance of the machine. Furthermore, cooling structures are currently uniformly distributed, which may not be the optimal solution for achieving optimal cooling performance [8]. In this context, this paper explores the state of the art in thermal management of electrical machines and focuses on the influence of distributed losses on temperature distribution and hot spot mitigation. A new method for designing distributed cooling structures is developed to tackle these challenges and enhance the efficiency and performance of water cooling in electrical machines.

## Enhancement of temperature distribution of cooling systems in Electrical machines

This chapter explores the enhancement of temperature distribution in cooling systems for electrical machines. At first the thermal losses are presented and conventional solutions for cooling are shown. Further on the influence of distributed losses on hotspots is shown using a testbench and fluid simulations. Based on the results of this investigation a method for distributing cooling structures, based on localized losses and cooling structure geometry is introduced. This method allows for a reduction of the temperature gradient for a planar test bench.

### *Losses and Cooling in Electrical Machines*

The losses in electric machines can be mainly divided into losses in the stator $P_{LS}$ and in the rotor $P_{LR}$. Additionally, there are mechanical losses $P_{LM}$ like air friction or bearing losses. The sum describes the total losses $P_L$ with Equation (1).

$$P_L = P_{LS} + P_{LR} + P_{LM} \quad (1)$$

The losses will vary in different operating points. A considerable part of the losses occur in the winding in the form of ohmic copper losses $P_{LS,Cu}$. The iron losses $P_{LS,Fe}$ depend on the electrical frequency [9], and the bearing losses depend on the mechanical load and speed. A possibility to dissipate the heat is to install a cooling jacket encasing the stator. Within this cooling jacket, a coolant fluid, i.e., water-glycol, is directed in different ways. An overview of typically used cooling jacket concepts is given in Figure 1. An often used concept is the spiraling flow path, depicted in a). Depending on the manufacturing, concepts like circumferential or axial meanders b) are used as well, i.e., in [10, 11]. Further on, other ideas like multiple inlets or outlets in different configurations are looked into [12].

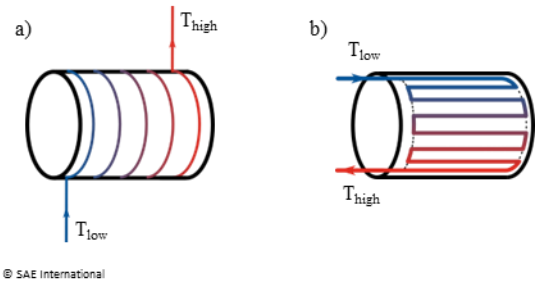


Figure 1 Flow concepts for cooling jackets (in accordance with [13])
a) Conventional Spiral b) Circumferential meander

Special cooling designs, like direct cooling embedded in the winding [14, 15] or oil spray cooling [7] are not considered in this paper as the focus of the research project is on cooling jackets.

### Boundary conditions (BC)

Further on boundary conditions for all CFD-calculations and analytical calculations are presented. The key data is given in Table 1 to 3. The CFD-calculations are generated using SOLIDWORKS Flow Simulation.

The electromechanical data for the target electric motor is shown in Table 1 with an S1-operating point and a peak operating point.

Table 1 Electromechanical data TI085
with kind courtesy of Fischer Elektromotoren GmbH

| Operating point | Torque Nm | Speed min-1 | Mechanical Power kW | Winding losses W | Power losses W |
|---|---|---|---|---|---|
| Continuous | 11.1 | 13,250 | 15.4 | 254 | 617 |
| Peak | 29.1 | 11,600 | 35.3 | 1,843 | 2,167 |

The main corresponding geometrical data for the motor can be taken from Table 2.

Table 2 Geometric data TI085
with kind courtesy of Fischer Elektromotoren GmbH

| Geometric parameters | | Value |
|---|---|---|
| Outer stator diameter | mm | 85 |
| Stator outer surface | mm² | 25,760 |
| Iron length | mm | 70 |
| Winding head length | mm | 9 |

For calculations regarding the cooling system, further boundary conditions are needed. For that reason, the following assumptions are made and used for the calculations within this paper.

- A coolant flow rate of 5 $l/min$ is the lower limit in industrial systems, here the values go up to 10 or 12 $l/min$ [6]; the lower limit of 5 $l/min$ was chosen as the motor is small in diameter with 85 $mm$
- The coolant inlet temperature is set to ambient temperature for reference, depending on different scenarios the inlet temperature can vary, where the upper limit usually is below 60 °C / 333 K.
- As thermal boundary, an adiabatic BC was chosen, as most of the heat in an integrated drive will be dissipated by the coolant flow.
- The sum of the losses $P_{LS}$ and $P_{LW}$ are approximated to 700 W assuming an S1-operating point and to 1,400 W for an intermittent S6-operating scenario.

Table 3 Boundary conditions for analytical and CFD calculations of this proceeding

| **Parameter** | **Value** | | |
|---|---|---|---|
| Coolant flow $\dot{Q}_c$ | 5 $l/min$ | | |
| Coolant inlet temperature $T_C$ | 293.15 $K$ | | |
| Back pressure $p_{amb}$ | 1,013 $mbar$ | | |
| Thermal boundaries | Adiabatic | | |
| Losses | $P_{LS}$ | $P_{LW}$ | $P_{\Sigma}$ |
| Continuous $P_{L,S1}$ | 400 W | 300 W | 700 W |
| Intermittent operation $P_{L,S6}$ | 800 W | 600 W | 1,400 W |

### Hot Spots in a Uniformly Flowed Through Cooling Jacket

Uniform coolant flows like presented in Figure 1 lead to a steady increase in the coolant temperature. This and distributed losses like a higher loss density in the winding head than the stator, can lead to hotspots. The results of a CFD simulation of a similar structure to Figure 1 b) is shown in Figure 2. It was performed to investigate a meandering design for the electric motor (Table 1 and Table 2) with the corresponding boundary conditions (Table 3). It can be seen that at the inlet the interface temperature between housing and stator is at 293.2 K and along the cooling channel the temperature rises. Additionally, there are hotspots at the flow redirection regions with about 310 to 312 K. As thermal derating has to be always performed regarding the highest temperatures, those single hotspots will be the main limiting factor. As there is no efficient heat sink for the isolated copper winding heads, which results in higher temperatures. The derating has to be done regarding the used insulation material, which is classified in temperature ranges. The use of a higher temperature class leads to higher costs [5].

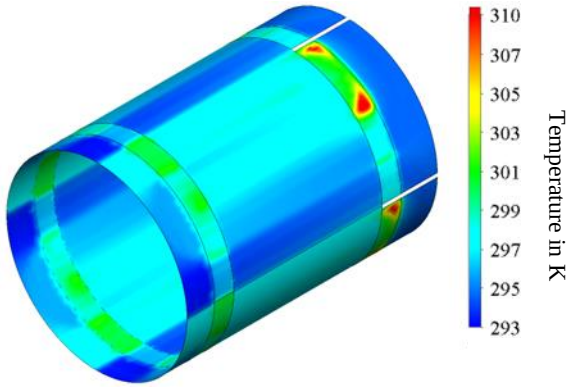


Figure 2 Interface temperature between stator and cooling jacket in a meandering design

### *Influence of Distributed Losses on Temperature Distribution*

Following these observations with the CFD simulation, a planar test bench was presented in a previous publication [13] of this research group. This test bench, shown in Figure 3, gives the possibility to measure the interface temperature (orange) in between a cooling channel with structures, and a segmented heating plate. It is used to investigate the influence of distributed losses on the temperature distribution along a cooling channel, which is the device under test (DUT). Further on, different DUTs with different cooling structures and cooling structure density distribution (DD) can be investigated and evaluated for their properties to reduce temperature gradients.

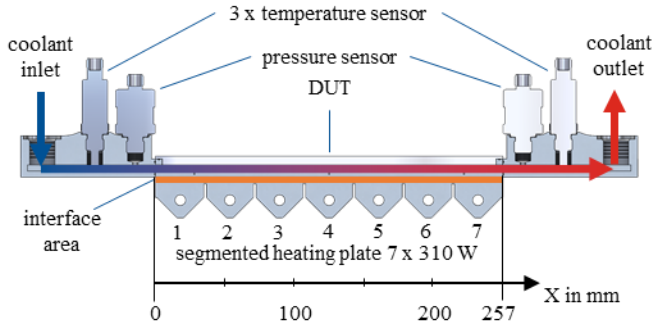


Figure 3 Test bench setup with temperature sensors in the interface area

One of the takeaways from the previous work is, that conventional cooling structures' main drawback is the uniform DD of cooling structures. A total thermal power $P_{\Sigma}$ of 1,400 W was induced in two scenarios, see Figure 4, which shows the used heat flux $\dot{Q}(x)$ in regard of the lengthwise position $x$ in the DUT. The blue line simulates the higher losses in regions like the winding head, whereas the red line represents uniformly distributed losses. This leads to a thermal gradient along the cooling channel.

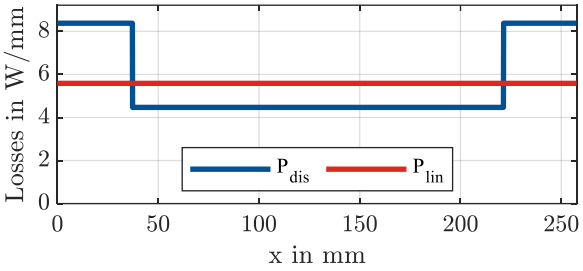

Figure 4 Heat flux along the DUT with channel width = 90 mm linear vs. distributed losses

This behavior can be seen in Figure 5. Here, a steel DUT without any additional cooling structures was placed on the heating plate. The linearly distributed losses lead to a quasi linear increasing interface temperature. When using a more realistic distribution with higher losses at the inlet and outlet and smaller losses in between, it can be seen that there are elevations of the temperature at the inlet of 12 K and 9 K at the outlet. The absolute temperature difference of the linearly distributed losses is 17.2 K and for the distributed losses it is 23.4 K.

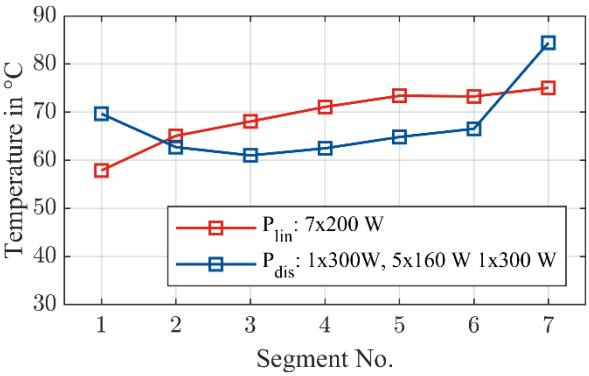

Figure 5 Measured interface temperature profile of steel DUT at 5 l/min linear (red) vs. distributed losses (blue)

## *Investigation of possibilities for reduction of temperature gradients*

The results from the linear test bench were analyzed and requirements for future cooling structures defined:

- Hotspots have to be addressed and reduced due to the fact, that thermal derating is performed in relation to the hottest part and insulation material properties
- Pressure loss should be minimized by applying cooling structures depending on the areas in need
- Thermal gradients should be reduced

### Investigation for the Use of Distributed Cooling structures

Those requirements lead to the idea of implementing cooling structures depending on the local boundary conditions. For this, some pre-tests were done and a method to distribute cooling structures was developed, which will be presented in this chapter.

***Iterative Design of a DUT for Proof of Concept***

At first, the distribution of cooling structures in a DUT was iteratively modified and analyzed using CFD-calculations. The approach in this procedure was to increase the number of pin fins in temperature hot spots, which mainly increases the usable surface area for heat dissipation. A quasi-linear temperature curve $T(x)$ was achieved by adjusting the number of pin fins segment wise. In Table 4, the resulting pin fin number for each segment is stated.

Table 4 Boundary conditions and resulting number of pin fins for iterative pin fin distribution

| **Segment** | **1** | **2** | **3** | **4** | **5** | **6** | **7** |
|---|---|---|---|---|---|---|---|
| Losses in Segment in W | 320 | 200 | 200 | 200 | 200 | 200 | 320 |
| Pin fins in segment | 33 | 27 | 27 | 27 | 33 | 39 | 57 |

Using CFD calculations and the aforementioned pin fin distribution, the results from Figure 6 were obtained. The empty channel has a maximum $\Delta T$ of $\sim 30\ K$ where the channel from "Iteration 4" has a $\Delta T$ of $\sim 5\ K$. As the boundary conditions were not fully defined for the iterative design, the total used power $P_\Sigma$ is $1640\ W$.

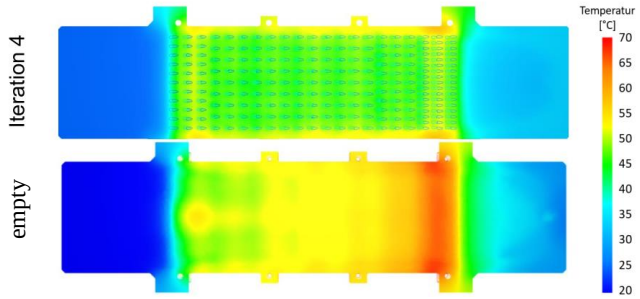

Figure 6 CFD calculations for the plain (leer) DUT and the iteratively designed DUT using CFD with deviating boundary conditions: $P_{Stator} = 1000\ W$, $P_{Windinghead} = 320\ W$, $P_\Sigma = 1640\ W$ [16]

The channel from "Iteration 4" was then manufactured using metal 3D printing and the DUT was put on the test bench and measurements were performed. For the measurement, the BCs as defined for this paper were used. For the empty channel, this results in a minimum temperature of 61 °C and a maximum temperature of 84.4 °C, or a temperature difference $\Delta T$ of 23.4 K. The minimum temperature for the channel with the DD of "Iteration 4" is 42.5 °C and the maximum is 51.7 °C. This is a difference of 9.2 K.

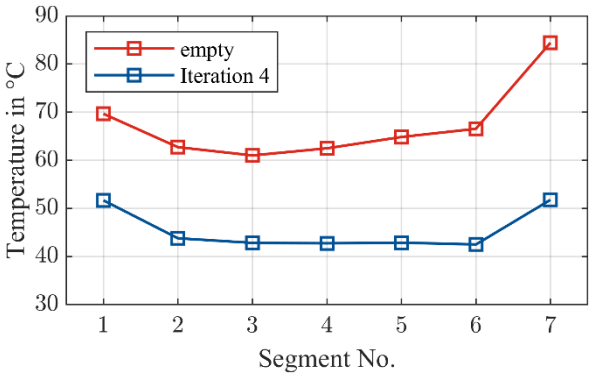


Figure 7 Temperature profile in steel DUT, 1,400W - distributed, 5 l/min empty channel (red) vs. distributed pin fins (blue)

***Modelling the Density Distribution for Isothermal Housing Temperatures***

As an iterative discrete design like previously shown is not a methodological approach, and takes up a lot of design time as well as calculation time, in the next part an analytical method to calculate the local surface heat transfer $\alpha(x) \cdot A(x)$, with the thermodynamic basics from [17] and [18], is presented.

Heat flux between a fluid and a solid can be modelled with (2), by consideration of the contact surface A, the temperature difference between the bulk fluid $T_F$ and the solid $T_S$, as well as the heat transfer coefficient $\alpha$.

$$\dot{Q} = \alpha \cdot A \cdot (\mathrm{T_S} - T_F) \tag{2}$$

One strategy to avoid hot spots in the electrical machine is to achieve a surface distribution $A$ along the cooling path $(x)$ in such a way that the surface temperature $T_S$ remains constant. The total heat flux $\dot{Q}$ from the housing can then be written as the heat flux per unit path length times the path length $\dot{Q}(x) = \frac{d\dot{Q}}{dx} x$. The bulk temperature rise of the fluid $T_F(x)$ along the fluid path is then proportional to the heat flux per unit path length $\frac{d\dot{Q}}{dx}$, as shown in Equation (3).

$$T_F(x) = T_{F,0} + \int_0^x \frac{1}{\dot{m} \cdot c_p} \frac{d\dot{Q}}{ds}\, ds$$

$$= T_{F,0} + \frac{d\dot{Q}}{dx} \cdot \frac{x}{\dot{m} \cdot c_p} \tag{3}$$

Here $\dot{m}$ is the fluid mass flow through the cooling channel and $c_p$ the heat capacity of the cooling fluid. Using the $\frac{d\dot{Q}}{dx}$ from Figure 4, the resulting $T_F(x)$ for the named boundary conditions for the DUT can be seen in Figure 8.

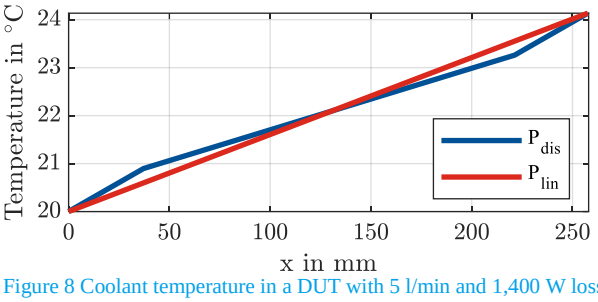


Figure 8 Coolant temperature in a DUT with 5 l/min and 1,400 W losses linear distribution (red) vs. distributed losses (blue)

Equation (4) can be developed by using the Equation (2) and (3) to calculate the product $\alpha(x)A(x)$ as a function of path length.

$$\alpha(x)A(x) = \frac{\frac{d\dot{Q}}{dx} \cdot x}{T_S - T_{F,0} - \frac{d\dot{Q}}{dx} \frac{x}{\dot{m} c_p}} \tag{4}$$

The equations above do not directly allow computing the necessary contact surface along the fluid path, since the heat transfer coefficient $\alpha$ remains unknown. Typical cooling channels of electrical machines do not exceed a characteristic hydraulic diameter $d_h$ 10 mm. In such a case, the flow in the channel is laminar and varies only a little with Reynolds number. Therefore, it seems legitimate to assume a constant Nusselt number and consequently a constant heat transfer coefficient $\alpha$ for the design of a cooling channel. For that reason, it is assumed further on that $\alpha(x)A(x)$, which then is mainly influenced by effective surface area, can be interpreted as $\alpha A(x)$.

Calculating the $\alpha A(x)$ for the boundary conditions, using the loss profile presented in Figure 4 and normalizing it to the minimum required surface will result in the normalized $\overline{\alpha A}(x)$ distribution given in Figure 9. It can be seen that for linearly distributed losses (red) the additionally required surface area is as well linearly increasing. The distributed loss profile results in a factor of 1.8-2 in the beginning and at the end.

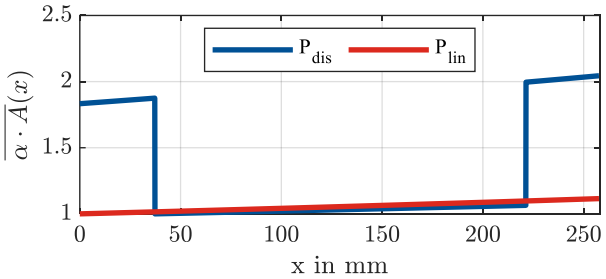


Figure 9 Normalized heat transfer and area $\overline{\alpha A}(x)$for a constant surface temperature
linear distribution (red) vs. distributed losses (blue)

***Cooling Structures and Effective Area Gain***

The resulting additional surface area has to be implemented within the cooling channel. For this, different structures are possible this can be i.e. multiple lamellas, round pins or even organic structures. Due to numerous previous works in the field of power electronics, in electric motors [8, 19, 20], but also own CFD calculations, the pin fin structure was chosen as the most suitable as pin fins have good cooling properties in regard of surface area and pressure drop. As well their DD can also be easily varied in all directions, lengthwise $(x)$ and in channel width.

The pin fin structure used further on was investigated by "Struve" in [21] and shows good properties in regard of manufacturability by 3D printing. It is shown that a pin fin with an aspect ratio $\varphi$

$$\varphi = \frac{R+r+a}{2 \cdot R} \tag{5}$$

between 1.5 and 2.5 is most suitable. Regarding manufacturing, the radius $r$ is the limiting factor.
The development and experimental investigations shown by Struve regarding the distance between fins, the alignment of the fins but also the angle of attack have also been performed independently by this workgroup using CFD calculations. The results are in good agreement, and a similar arrangement is used in the further work.

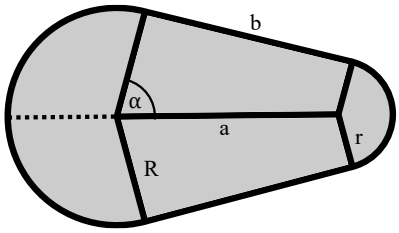


Figure 10 Pin fin profile with $\varphi = 2$ in accordance with [21]

It is important to properly calculate the base area of a single pin fin in order to determine the number of pin fins needed for the desired DD. According to "Struve" the base area can be calculated by:

$$A_{base} = R^2 \cdot (\pi - \alpha) + (R + r) \cdot a \cdot sin(\alpha) + r^2 \cdot \alpha \tag{6}$$

For this, a helper angle using Equation (7) can be calculated.

$$\alpha = \cos^{-1}\left(\frac{R-r}{a}\right) \tag{7}$$

The distance $a$ of the center points of the big and small arc are necessary and can be calculated by Equation (8).

$$a = R \cdot (2\varphi - 1) - r \tag{8}$$

The base area is not sufficient for the further steps of calculating the number of pin fins, needed to meet the desired DD given by the local $\overline{\alpha A}(x)$. For this the shell surface of a pin fin is needed as well, to calculate the effective area gain $A_{gain}$.
For that reason, the pre-work of "Struve" was followed up by Equation (9) to at first calculate the total circumference $C_{total}$.

$$C_{total} = C_R(R, \alpha) + C_r(r, \alpha) + 2 \cdot b \tag{9}$$

For this, the length of the arcs $C_R$ and $C_r$ have to be determined using Equation (10).

$$C_R = \pi \cdot R \cdot \left(1 + \frac{2 \cdot \alpha}{180°}\right); C_r = \pi \cdot r \cdot \left(1 - \frac{2 \cdot \alpha}{180°}\right) \tag{10}$$

The length of the connecting straight line $b$ can be determined by Equation (11)

$$b = \sqrt{[(R - r) \cdot \cos(\alpha) - a]^2 + [(R - r) \cdot \sin(\alpha)]^2} \tag{11}$$

Using the height $h$ of the channel, the additionally effective surface gain $A_{gain}$ can be calculated by Equation (12). As the base area $A_{base}$ is no longer directly in contact with the coolant fluid, it has to be subtracted. It is assumed at this point that the top of the channel has no significant contribution to the thermal dissipation, which was also observed in the pre-tests. For that reason, $A_{base}$ is only subtracted once.

$$A_{gain} = h_{channel} \cdot C_{total} - A_{base} \tag{12}$$

This effective surface area gain can then be used, to adapt the local DD to meet the required local $\overline{\alpha A}(x)$.

***Design of an optimized DUT***

The calculation of the corresponding pin fin distribution needs some further boundary conditions like, i.e., horizontal and vertical distances between pin fins, to properly place the pin fins. Here it has to be kept in mind, that the pin fins have to be placed at discrete positions along the channel, with lengthwise and widthwise distance, as well as distance to other walls. The parameters are also based on "Struve's" investigations and described in Table 5.

Table 5 Boundary conditions for pin fin distribution based on [21]

| Parameter | Value |
|---|---|
| Top Radius | $R = 1.2\ mm$ |
| Bottom radius | $r = 0.5\ mm$ |
| Phi | $\varphi = 2$ |
| Distance between pin fin positions | $l_s = 1.5 \cdot l = 7.5\ mm$ |
| Distance between pin fins | $w_{distance} = 1.5 \cdot 2 \cdot R$ |
| Channel width | $w_{ch} = 90\ mm$ |
| Channel height | $h_{ch} = 1\ mm$ |

The length of a single pin fin can be calculated using Equation (13).

$$l_{pf} = R + r + a \tag{13}$$

The distance between the center of the pin fins multiplied by a distance factor results in channel segments with length $l_s$.The base area of a section $A_{ch,s}(x)$, where the pin fins are placed, is given by Equation (14).

$$A_{ch,s}(x) = w_{ch}(x) \cdot l_s \tag{14}$$

Using the previously calculated normalized $\overline{\alpha A}(x)$ from Equation (7) for a discrete position $x$, the required numbers of pin fins for the section $N_s(x)$, can be determined by:

$$N_s(x) = (\overline{\alpha A}(x) - 1) \cdot \frac{A_{ch,s}(x)}{A_{gain}} \tag{15}$$

As this calculation will result in non-natural numbers and pin fins, can only be placed in natural numbers, the result from $N_s$ either has to be rounded up or down. As positions for the pin fins discrete locations along the channel $x$ with distance $l_s$ are used. When rounding up to the next closest integer, the distribution of $N_s(x)$ shown in Figure 11 is obtained, with the orange line being the geometric limit for number of Pinfins in a segment. The division of this number by the volume of the cooling channel results in the ideal DD.

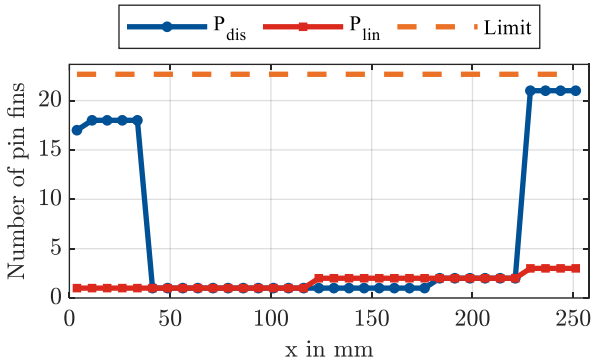

Figure 11 Pin fin distribution $N_s(x)$ for a linearly distributed losses (red) and distributed losses (blue) with geometric parameters from Table 5

***CFD Simulation of the Optimized DUT***

The CFD results of a DUT with an empty channel and distributed losses are shown. As previously stated, the temperature at the inlet and outlet is elevated, with the inlet being at about 312 K and the outlet being at 316 K. The region in between is cooler with a minimum temperature of 303 K. This results in a temperature difference of 13 K within the DUT.

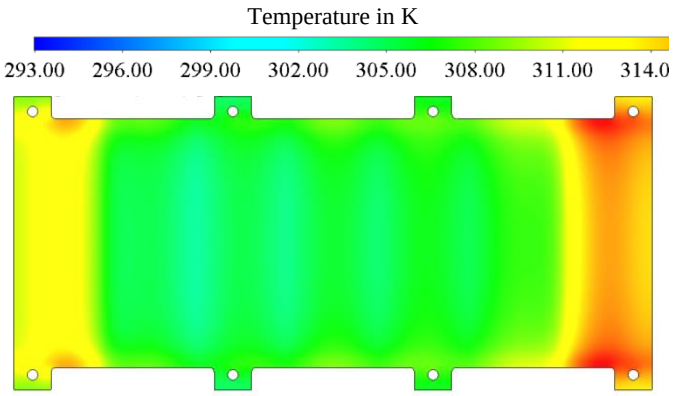

Figure 12 Linear DUT without cooling structure, $P_\Sigma = 1{,}400\ W$
Fluid cells 388,224; Solid cells 575,724

In Figure 13, the CFD of a DUT with the DD from Figure 11 is shown. As the required DD in the middle section is quite low, only a single pin fin per section is inserted. With this DD, the temperature spread within the DUT improves significantly compared to Figure 12, with 293.8 K at the inlet and 298.9 K at the outlet. The temperature gradient within the DUT can be reduced from 13 K to 5 K.

Comparing this distribution to the iterative design “Iteration 4” in Figure 7 also clarifies the temperature elevations in the iterative design, as there are more pin fins within the middle section, inserting a disbalance of the analytical description.

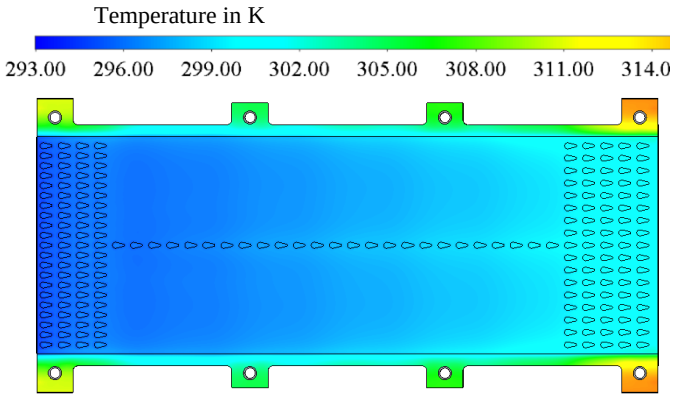

Figure 13 Linear DUT with distributed cooling structure according to Figure 11, $P_\Sigma = 1{,}400\ W$, Fluid cells 682,608; Solid cells 938,005

## *Implementation of the Distributed Cooling Structure in an EM Housing*

The previously shown method can be used for any channel, as long as the loss profile along the channel can be created. This can be done by using CAD-Software, from which such a profile can be exported. But for complex geometries, as i.e. meandering designs, this can be difficult. Another problem occurring with more complex geometries is the need to manually design the distribution using CAD or do a structure dependent intensive implementation of a generative design approach.

### Design of a two layer cooling jacket

For this reason, a design was developed, which allows to describe the loss profile as a function along the rotary axis, as shown in Figure 14 and let the coolant flow in the same direction. The method for pin fin distribution then can be used analog, as used in the previous chapter with the planar DUT. In the design, the cooling jacket is divided into an inner and outer jacket. In the inner jacket, the pin fins can be placed using generative design approaches. The outer jacket is used to return the coolant fluid to the same side as the inlet. This was done as one requirement in the project is to install the coolant connections on the same side of the housing. This can be implemented depending on the needs of the application.

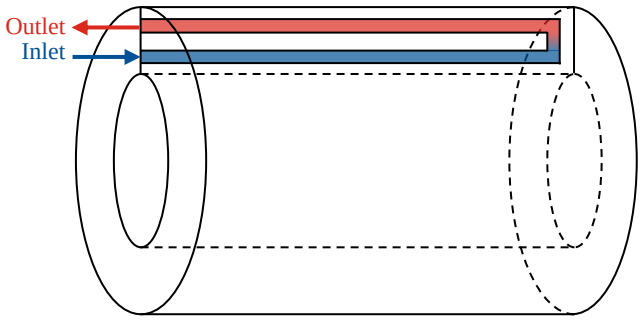

Figure 14 Two layered cooling jacket with inside distributed cooling structures

The inlet structure is designed as well rotationally symmetric, to keep pressure losses low and equally distribute the coolant, as can be seen in Figure 15. The white occurring areas represent walls within the housing, as physical connections are needed for stability and transmission of forces.

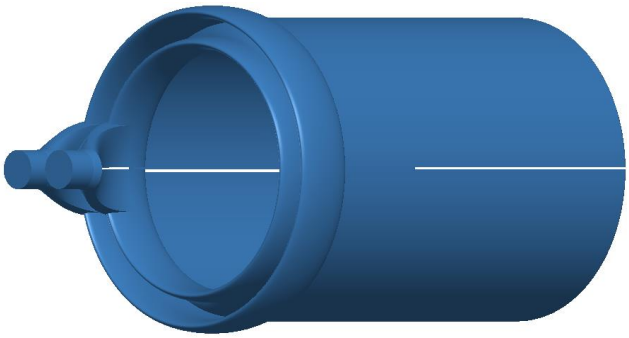

Figure 15 Two layered cooling jacket with inside distributed cooling structures

***Evaluation of the Concept to Minimize Heating of the Inlet***

As a two layered cooling jacket, as shown in Figure 14, can also be interpreted as a heat exchanger with counterflow principle, one can argue that the inlet coolant will be heated by the returning warm coolant fluid. This problem can be looked at by using the NTU-method presented by "Lienhard" in [22]. Here, the effectiveness of a heat exchanger can be quantized by comparing the actual heat transfer to the maximum heat capacity of the coolant. A small NTU value will result in a low efficiency of a heat exchanger. Which in this case is the desired requirement.

Using the case of 1,400 W of losses, a wall temperature of 35 °C and an average coolant temperature of 22 °C, the averaged $\alpha \cdot A$ is equal to 107 $W/K$. With a volumetric flow rate of 5 $l/min$ and the thermal capacity of water, the resulting $\dot{m} \cdot c_p$ is 348.12 $W/K$. Calculating the NTU with these values we get:

$$NTU = \frac{U \cdot A}{C_{min}} \sim \frac{\alpha \cdot A}{\dot{m} \cdot c_p} = \frac{107 \frac{W}{K}}{348.12 \frac{W}{K}} = 0.307 \qquad (16)$$

As the goal is not to create a heat exchanger but to cool the surface, the two layer concept fulfills the requirements in this perspective.

***Implementation of the Distributed Cooling Structure in the Two Layered cooling Jacket***

To implement the previously described method for pin fin distribution, the loss distribution along the cooling channel has to be defined, see Figure 16. In this investigation, it can be observed that the losses per unit length are higher compared to the linear DUT under similar operating conditions. This disparity can be attributed to the direction of flow along the surface. The observed flow direction in the examined case is predominantly aligned with the shorter rotary axis (88 mm), whereas in the linear device, the flow direction is more aligned with the surface corresponding to the radial mantle surface (256 mm). It will be beneficial to express future losses in W/mm$^2$ to reduce this misinterpretation.

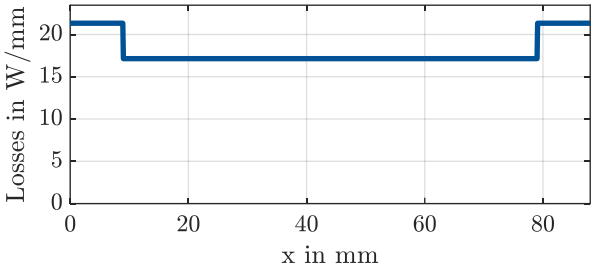


Figure 16 Loss profile along the cooling jacket

From the loss profile at first the temperature of the coolant is calculated and then the normalized $\overline{\alpha A}(x)$, shown in Figure 17, is generated. It can be seen that in the areas of the winding head a factor of approx. 1.25 - 1.3 is needed.

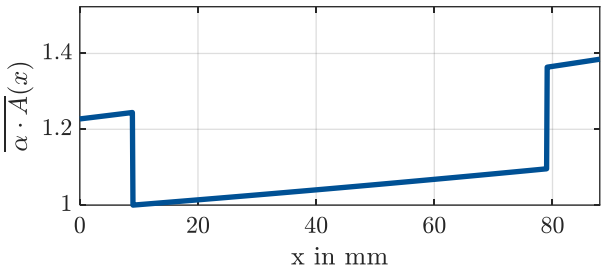


Figure 17 Resulting $\overline{\alpha A}(x)$ of the cooling channel with loss profile from Figure 16

This leads to the resulting number of needed pin fins for the cooling channel, which is shown in Figure 18. The factor of 1.25 results in 61 pin fins in the first section. This is because the surface area gain $A_{gain}$ for a single pin fin is small, due to a cooling channel height of only 1 mm. In the last section, where the second winding head is located, it results in a total number 80 pin fins.

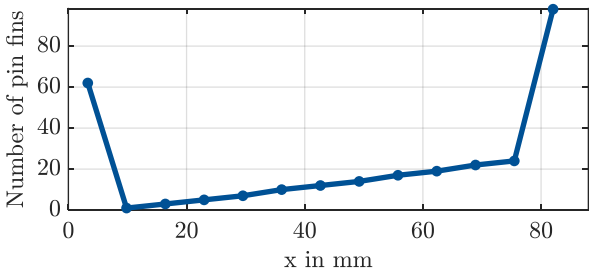


Figure 18 Resulting desired number of pin fins for the $\overline{\alpha A}(x)$ from Figure 17

## CFD Calculations of the Two Layer Cooling Jacket with Distributed Cooling Structures

For reference, the two layered cooling jacket is simulated without pin fin structures. This leads to increased hotspots, with 310.8 K especially near the winding head, as can be seen in Figure 19. The temperature difference $\Delta T$ along the surface is 17.5 K.

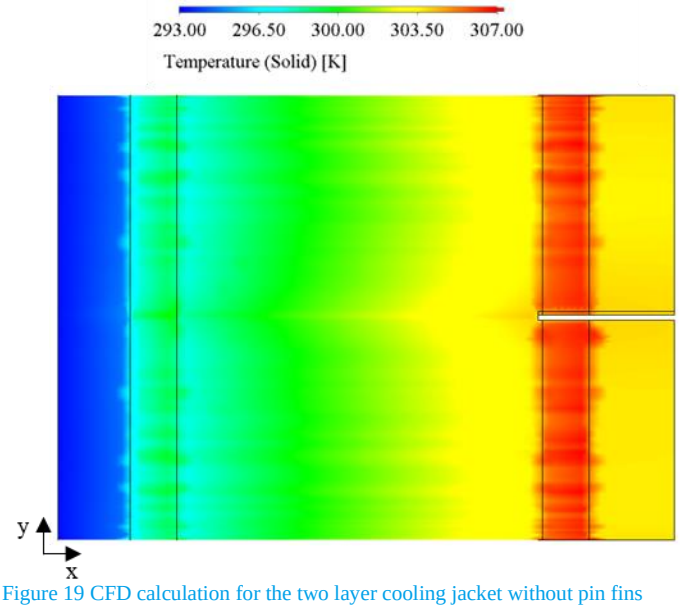

Figure 19 CFD calculation for the two layer cooling jacket without pin fins
Fluid cells 273,015; Solid cells 378,733

The cooling jacket with the pin fin DD from Figure 18 was simulated and the temperature distribution in Figure 20 was achieved. Based on the observed plot, it can be inferred that the temperature distribution is not as anticipated. Contrary to expectations, the implementation of the distributed pin fins, does not effectively mitigate the uneven distribution of temperatures in this cooling jacket design. Despite the implementation, only a minor improvement, in the reduction of the maximum temperature to 308.4 K is achieved.

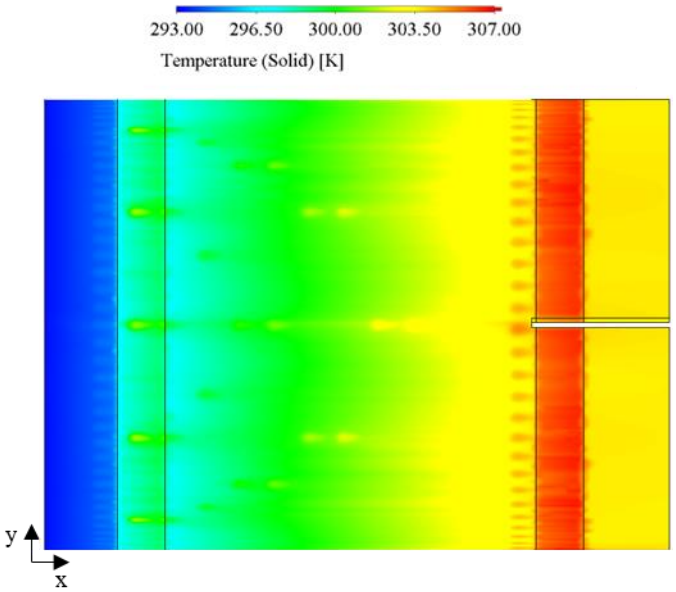

Figure 20 CFD calculation for the two layer cooling jacket with pin fins
Fluid cells 1,107,847; Solid cells 1,708,322

## Summary/Conclusions

This scientific paper focuses on addressing hotspots and temperature gradients in cooling systems for electrical devices. An analytic approach is proposed to estimate the required distribution of pin fins using the normalized $\overline{\alpha A}(x)$ when a loss profile $\dot{Q}(x)$ is available. By utilizing this approach along with knowledge of the cooling structure geometry – in this case the pin fin geometry - a distribution that theoretically achieves a uniform interface temperatures to the stator is calculated using the specific heat transfer capability of the chosen structure. CFD simulations have been performed to validate the effectiveness of this method.

By applying the developed method to a linear DUT it was possible to reduce the temperature gradient. In an iterative design, the gradient was dropped down to 9 K and with the analytic method in a CFD calculation down to 5 K. A cooling jacket, with the possibility to implement the pin fins using generative design, was specifically designed. The developed method was subsequently applied to the jacket. The implementation of distributed pin fins did not yield the desired reduction in the temperature gradient. The setup is assumed to have a negative outcome due to the small channel height of 1.5 mm, as well as the area of redirection, which is not yet optimized, and leading to inconstant flow speed. Nonetheless the good results from the planar DUT, can i.e. be transferred to the development of cooling systems in batteries for BEVs or in a smaller variant in the heat sinks for power electronics.

Several key observations have been made during the study. First, it is recommended to calculate the loss density in W/mm² instead of W/mm. The further development should as well better define the DD in regard of cooling volume. Secondly, the effective area gain is found to be linearly dependent on the channel height, which may result in effective area loss based on the pin fin to channel height ratio. Additionally, it was observed, that the small EM size in regard to the cooling structure geometry (length, width) will lead to the problem, that a fine granular DD is hard to achieve. In the presented case, only one row of pin fins fitted in the winding head section. Furthermore a bigger channel height than 1.5 mm will lead to disproportional cooling channels in comparison to the stator diameter.

For future research, the authors suggest at first the investigation of the unexpected findings of the pin fin DD in the cooling jacket, especially the influence and limits for the proposed method regarding channel height. Further on the use of different pin fin geometries with certain channel parameters can be evaluated, as they may provide better effective area gain compared to the used pin fins. Optimizing geometric parameters such as pin fin dimensions, distances between pin fins, and channel height is also identified as an important area for further exploration. Furthermore, studying different cooling structures, i.e. dimples with a possibility to adapt the thermal transfer coefficient $\alpha(x)$ and their arrangements, as well as considering time-varying load cycles, are recommended to gain a more comprehensive understanding of the cooling system's performance and efficiency. These future investigations will contribute to the development of improved cooling strategies for electrical devices.

# References

1. “Vehicles and fleet | European Alternative Fuels Observatory,” https://alternative-fuels-observatory.ec.europa.eu/transport-mode/road/european-union-eu27/vehicles-and-fleet, May 8, 2023.
2. Geimer, M. (ed.), “Hybride und energieeffiziente Antriebe für mobile Arbeitsmaschinen: 9. Fachtagung, Karlsruhe, 28. Februar 2022,” Karlsruher Schriftenreihe Fahrzeugsystemtechnik, Band 106, KIT Scientific Publishing, Karlsruhe, ISBN 9783731512608, 2023.

3. Wrobel, R., “A technology overview of thermal management of integrated motor drives – Electrical Machines,” *Thermal Science and Engineering Progress* 29:101222, 2022, doi:10.1016/j.tsep.2022.101222.
4. Liu, H., Wrobel, R., Ayat, S., and Zhang, C., “Coupled Electromagnetic and Thermal Design-Optimisation of a Traction IPM Machine with High- Torque Overload Capability,” *2018 XIII International Conference on Electrical Machines (ICEM)*, 2018 XIII International Conference on Electrical Machines (ICEM), ISBN 2381-4802:2647–2653, 2018.
5. Hemsen, J. and Eckstein, L., “A Thermal Model for the Comparison of Cooling Concepts of Synchronous Machines for Traction Applications,” *SAE Technical Paper Series*, SAE Technical Paper Series, Conference on Sustainable Mobility, SEP. 25, 2022, SAE International400 Commonwealth Drive, Warrendale, PA, United States, 2022.
6. Gronwald, P.-O. and Kern, T.A., “Traction Motor Cooling Systems: A Literature Review and Comparative Study,” *IEEE Transactions on Transportation Electrification* 7(4):2892–2913, 2021, doi:10.1109/TTE.2021.3075844.
7. Liu, C., Gerada, D., Xu, Z., Chong, Y.C. et al., “Estimation of Oil Spray Cooling Heat Transfer Coefficients on Hairpin Windings With Reduced-Parameter Models,” *IEEE Transactions on Transportation Electrification* 7(2):793–803, 2021, doi:10.1109/TTE.2020.3031373.
8. Feikus, F.J., Bernsteiner, P., Gutiérrez, R.F., and Łuszczak, M., “Weiterentwicklungen bei Gehäusen von Elektromotoren,” *MTZ Motortech Z* 81(3):42–47, 2020, doi:10.1007/s35146-019-0180-5.
9. Krings, A. and Soulard, J., “Overview and Comparison of Iron Loss Models for Electrical Machines,” 2010.
10. Acquaviva, A., Wallmark, O., Grunditz, E.A., Lundmark, S.T. et al., “Computationally Efficient Modeling of Electrical Machines With Cooling Jacket,” *IEEE Trans. Transp. Electrific.* 5(3):618–629, 2019, doi:10.1109/TTE.2019.2936122.
11. Huber, A., Pfitzner, M., Nguyen-Xuan, T., and Eckstein, F., “Effiziente Strömungsführung im Wassermantel elektrischer Antriebsmaschinen,” *ATZelektronik* 8(6):478–485, 2013, doi:10.1365/s35658-013-0370-8.
12. Yang, X., Fatemi, A., Nehl, T., Hao, L. et al., “Comparative Study of Three Stator Cooling Jackets for Electric Machine of Mild Hybrid Vehicle,” *2019 IEEE International Electric Machines & Drives Conference (IEMDC): May 12-15, 2019, Westin San Diego, San Diego, CA*, IEEE, [Piscataway, New Jersey], ISBN 978-1-5386-9350-6:1202–1209, 2019.
13. Ellenrieder, C., Reick, B., Kaufmann, A., and Geimer, M., “Optimization of Water Cooling for High Power Density Electrical Machines,” *SAE Technical Paper Series*, SAE Technical Paper Series, Conference on Sustainable Mobility, SEP. 25, 2022, SAE International, 400 Commonwealth Drive, Warrendale, PA, United States, 2022.
14. Schiefer, M. and Doppelbauer, M., “Indirect slot cooling for high-power-density machines with concentrated winding,” *2015 IEEE International Electric Machines & Drives Conference (IEMDC)*, 2015 IEEE International Electric Machines & Drives Conference (IEMDC), Coeur d'Alene, ID, 10.05.2015 - 13.05.2015, IEEE, ISBN 978-1-4799-7941-7:1820–1825, 2015.
15. Wrobel, R., “A technology overview of thermal management of integrated motor drives – Electrical Machines,” vol. 29, 2022.
16. Heinz, L., Ellenrieder, C. Supervisor, and Kaufmann, A. Supervisor, “Systematische Untersuchung von Kühlstrukturen in wassergekühlten elektrischen Maschinen,” 2022.
17. Bergman, T.L. and Lavine, A.S., “Incropera's principles of heat and mass transfer,” 8th ed., Wiley, Hoboken, NJ, ISBN 1119382912, 2017.
18. Marek, R. and Nitsche, K., “Praxis der Wärmeübertragung: Grundlagen - Anwendungen - Übungsaufgaben ; mit 54 Tabellen, 50 vollständig durchgerechneten Beispielen sowie 136 Übungsaufgaben mit ausführlichen Lösungen auf CD,” 4th ed., Fachbuchverlag Leipzig im Carl Hanser Verlag, München, ISBN 9783446444997, 2015.
19. Karras, N., “Optimierung der Wärmeabfuhr eines Fahrzeug-Elektromotors und Auswirkungen auf den Gesamtkühlkreislauf,” Dissertation, Universität Stuttgart, Stuttgart, 2017.
20. Al-Neama, A.F.M., “Serpentine Minichannel Liquid-Cooled Heat Sinks for Electronics Cooling Applications,” Dissertation, The University of Leeds, Leeds, 2018.
21. Struve, A., “Generatives Design zur Optimierung additiv gefertigter Kühlkörper,” Springer Berlin Heidelberg, Berlin, Heidelberg, ISBN 978-3-662-63070-9, 2021.
22. Lienhard, IV, J. H., J.I. and Lienhard, J.V., “A Heat Transfer Textbook,” 5th ed., Phlogiston Press, Cambridge, MA, 2020.

## Contact Information

Christoph Ellenrieder, M.Sc. – christoph.ellenrieder@rwu.de
Ravensburg-Weingarten University
88250 Weingarten
Germany

## Acknowledgments

"This Project is supported by the Federal Ministry for Economic Affairs and Climate Action (BMWK) on the basis of a decision by the German Bundestag."

## Definitions/Abbreviations

| | |
|---|---|
| **EM** | Electric motor |
| **IMD** | Integrated motor drive |
| **DD** | Density distribution |
| **BC** | Boundary condition |
| **CFD** | Computational fluid dynamics |

ISSN 0148-7191
https://saemobilus.sae.org/content/2023-24-0126